A flux monitoring method for easy and accurate flow rate measurement in pressure-driven flows

Article *in* Lab on a Chip · February 2012

DOI: 10.1039/c1lc20480g · Source: PubMed

4 authors, including:

Anne-Laure Biance
French National Centre for Scientific Research
49 PUBLICATIONS **914** CITATIONS
SEE PROFILE

Christophe Ybert
French National Centre for Scientific Research
67 PUBLICATIONS **2,769** CITATIONS
SEE PROFILE

Lyderic Bocquet
Ecole Normale Supérieure de Paris
199 PUBLICATIONS **9,602** CITATIONS
SEE PROFILE

Lab on a Chip

Cite this: *Lab Chip*, 2012, **12**, 872

www.rsc.org/loc

TECHNICAL INNOVATION

A flux monitoring method for easy and accurate flow rate measurement in pressure-driven flows†

Alessandro Siria,* Anne-Laure Biance, Christophe Ybert and Lydéric Bocquet

Received 2nd June 2011, Accepted 8th November 2011
DOI: 10.1039/c1lc20480g

We propose a low-cost and versatile method to measure flow rate in microfluidic channels under pressure-driven flows, thereby providing a simple characterization of the hydrodynamic permeability of the system. The technique is inspired by the current monitoring method usually employed to characterize electro-osmotic flows, and makes use of the measurement of the time-dependent electric resistance inside the channel associated with a moving salt front. We have successfully tested the method in a micrometer-size channel, as well as in a complex microfluidic channel with a varying cross-section, demonstrating its ability in detecting internal shape variations.

The two main approaches for driving or pumping fluids in micro- and nano-fluidic channels are pressure-driven (Poiseuille), and electrically driven, electro-osmotic flow (EOF).[1,2] EOF is an interfacially driven flow generated by electrical forcing in the Debye layer near the walls. It has many advantages as pointed out by the numerous literature on the subject, from the most fundamental study of electro-osmotic flow[3–6] up to applications on living cells.[7] While EOF is easy to integrate in micro- or nano-fluidics devices, it is however strongly dependent on the surface characteristics and furthermore leads to relatively slow flows (10–100 μm s^{-1}), unless very high voltage is applied,[8–12] then inducing undesirable large thermal effects in the system.[12] As a matter of fact, pressure-driven flow remains a method of choice for many applications. It is nowadays easily integrated in multilayer microfluidics systems,[13] allowing faster movement in micro and nanochannels. It is driven in the bulk of the fluid, leading to a parabolic Poiseuille flow profile in the materials, in contrast to the plug-like velocity profile associated with EOF.

In both driving methods, measuring quantitatively the flow rate in the channel is crucial for both fundamental studies and applications. While EOF provides information on the surface zeta potential, the flow rate in pressure-driven flows allows for a measurement of the hydrodynamic permeability of the channel, and *in fine* of its transverse size.

Over the years the community has developed various techniques to probe flow rates in channels. While for large pipes, say in the millimeter range, the flow rate can simply be measured from the weight of the outcoming liquid, measuring the permeability of micron-size channels – or less – remains challenging. Direct flow field measurement, using *e.g.* micro particle image velocimetry (μ-PIV)[11,14] provides much insight into the flow profile, however at the expense of a heavy instrumentation and sophisticated analysis. An alternative flow transducer technique was proposed recently,[15] based on the measurement of electrochemical admittance of a pair of gold electrodes integrated in a microchannel.[15,16] A disadvantage of such a technique however is that it requires the introduction of electrodes into the microchannel to probe flow. In contrast, EOF allows for a much simpler and efficient technique, the so-called *current monitoring* technique.[8–12] Under EOF the interface between two salt solutions with slightly different ion concentrations propagates through the channel as a front and the electro-osmotic velocity is measured *via* the time-dependence of the current through the channel with variable resistance. This method can be developed at low-cost, and is accordingly widely used in the microfluidic community to probe the zeta potential of channel surfaces.[3,9] In this paper, we show that the current monitoring method can be extended to probe the flow rate under pressure-driven flow, thereby realizing a 'flux monitoring' technique. We have first validated the technique in a simple micro-capillary. Then we show that it can be used as a diagnostic tool to probe channels with varying cross-sections.

The general methodology follows that of the classical current monitoring technique used for EOF. The channel and its reservoirs are initially filled with a salt solution with a given salt concentration. Then the inlet reservoir is flushed with a new salt solution with a slightly different salt concentration and a flow is induced by applying a pressure drop between the two reservoirs. We then measure the current induced in the channel by a low difference of potential applied between the reservoirs. The averaged flow rate can be deduced from the transition time needed for the current to saturate to its final value. Under the hypothesis that the concentration front is moving at the average fluid velocity, the time to reach the plateau is expected to be

LPMCN, UMR 5586, CNRS, Université Claude Bernard Lyon 1, 43 bd du 11 Novembre 1918, 69622 Villeurbanne, France. E-mail: alessandro.siria@univ-lyon1.fr

† Electronic supplementary information (ESI) available. See DOI: 10.1039/c1lc20480g

$\tau = L/\bar{V}$, with L the channel length and $\bar{V}$ the averaged velocity in the channel, defined in terms of the flow rate Q and cross-section $\mathcal{A}$ of the channel, $\overline{V} = Q/\mathcal{A}$. As we show in the ESI,† this estimate is actually very robust, even when the salt diffusion–convection dynamics are taken into account. Introducing the hydrodynamic permeability of the channel K_{hyd}, which we define here as $\bar{V} = K_{hyd}(-\Delta P/L)$, one deduces accordingly:

$$\tau = \frac{L^2}{K_{hyd}|\Delta P|} \quad (1)$$

Using Hagen–Poiseuille expression for K_{hyd} in a cylindrical channel with radius R, one has

$$\tau = \frac{L^2 8\eta}{\Delta P R^2}, \quad (2)$$

where η is the fluid viscosity. The flux monitoring thus allows for a measure of the channel hydrodynamic permeability K_{hyd}.

We first explore this procedure in a benchmark experiment using a commercial silica capillary (Polymicro) with length $L \approx 6$ cm and a radius $R \approx 1$ μm. All the different techniques introduced previously,[11,14–16] dealing with the measurement of pressure-driven flow, cannot be applied to such a kind of microchannel, therefore showing the advantage of the flux monitoring technique presented here.

This channel connects two reservoirs (1,2) filled with KCl salt dissolved in deionized water at different concentrations (c_1, c_2), see Fig.1. A pressure drop $\Delta P = P_1 - P_2$ is applied between the extremities of the capillary. The excess pressure is applied in one reservoir by connecting it to an air flow controller supplied by an 8 bar compressor. The pressure is controlled *via* a voltage-commanded valve (SMC Corp.), allowing an excess pressure up to 2.17 bar. The pressure applied in the reservoir has been calibrated *via* a Hg hydrostatic column. The ionic resistance of the channel is recorded *versus* time by applying a voltage difference and by measuring the current *via* a home-made low-noise I/V converter (allowing a resolution within 1 pA). Two Pt electrodes are connected to the reservoirs. A voltage difference is applied at the electrodes *via* an I/O digital analogic converter (*NI*) controlled by a home-made LabView set-up. The whole set-up is placed in a Faraday cage. The resistance of the channel is deduced from typical I/V curve. If c_1 is larger than c_2, one can observe that the resistivity of the channel is increasing with time before reaching a plateau, as shown in Fig.2. Varying salt concentrations c_1 and c_2, induces different values for the plateaus, see Fig. 2, but does not affect the time needed to reach the plateau. Furthermore the

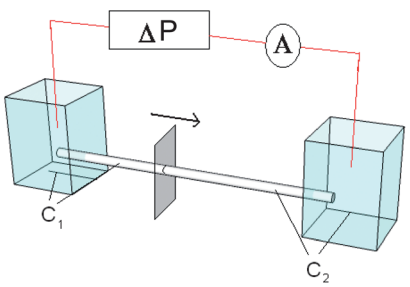

Fig. 1 Illustration of the experimental set-up developed for the electrokinetic measurement.

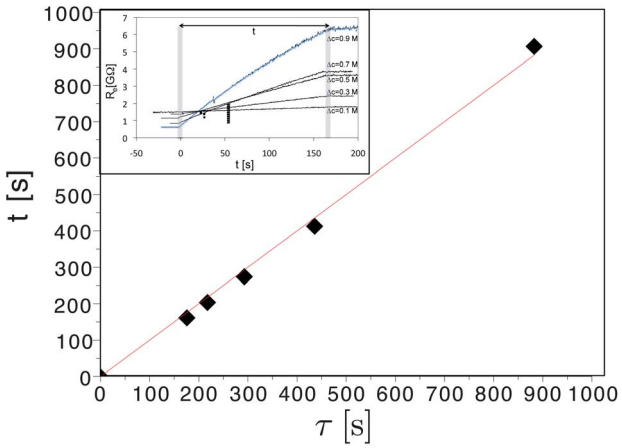

Fig. 2 Experimental transport time t (s) measured for different applied pressure *versus* its theoretical prediction τ, in eqn (2). The salt concentration is 0.1 M and τ is varied by changing the overpressure between the two reservoirs from 430 mbar to 2.17 bar. The straight line has a slope of 1. In the inset, resistance of the channel ($R = \Delta V/I$) *versus* time t with a constant 10 V applied voltage for different KCl concentration differences. $c_1 + c_2$ remains constant and equal to 1.1 M. Applied pressure is 2.17 bar. The time t between the two plateaus remains constant.

variations of the channel resistance with time are shown to be linear. These results allow to test the simple estimate proposed in eqn(2) for the transition time, here measured for various pressure drop ΔP. Experimentally we defined this time with a precision better than 1%, by intersecting the slopes of resistance and the plateaus. In Fig. 2, we plot the measured time *versus* the expected Poiseuille–Hagen prediction in eqn(2), showing an overall very good agreement. In this estimate we used $R = 1040$ nm for the channel hydrodynamic radius, in full agreement with the data given by the company description. The main uncertainty here results from applied pressure accuracy. These results do show that the present 'flux monitoring' technique, initially developed to probe EOF, is able to provide at low experimental cost a confident measurement of the flow rate under pressure-driven flow. As we detail in the ESI,† the range of operation of this method is broad in terms of parameters (channel diameter to length aspect ratio, pressure drop and applied voltage), making the method robust and versatile.

Beyond the permeability measurements, we now show that the above approach can be also used as a simple diagnostic method to probe the shape of a channel. The general idea is that the time-dependent electric resistance is a direct function of the cross-sectional area $\mathcal{A}(z)$ of the channel along its length z. The time dependence of the electric resistance as the salt front travels along the channel is therefore a direct signature of the shape variations. This idea can be rationalized on the basis of the Taylor–Aris description,[17] see ESI.† The main limiting factor for the application of the method in channels with varying sizes is the occurrence of transients associated with the diffusion of the salt over the varying lateral size of the channels. This suggests that the method is not suited to probe strong variations in the cross-section.

In order to illustrate this approach to probe shape variation, we have considered the flux-monitoring response of a benchmark PDMS microchannel with a varying section as depicted in Fig. 3:

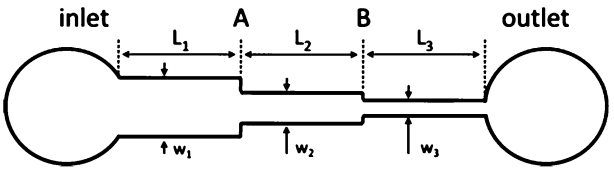

Fig. 3 Sketch of the microfluidic channel with a varying channel width. The channel width is: 200 μm; 150 μm; 100 μm. The channel depth is constant and equal to 50 μm.

it consists of a microfluidic channel with three different sections $w_1 = 200$ μm, $w_2 = 150$ μm, $w_3 = 100$ μm with respective lengths $L_1 = 8.4$ cm, $L_2 = L_3 = 6.7$ cm and a constant depth $d = 50$ μm. This design exhibits sharp variations in the cross-section, which, as discussed above, is not favorable to the method. However, we show below that the method provides much information on the channel shape even in such stringent conditions. The PDMS channel has been deviced using standard lithography techniques. First, a 50 micrometer layer of a UV-sensitive solid film is deposited, exposed to UV and heated at 80 °C on a glass lamella. On this "adhesive" layer, a second layer of the film is deposited and exposed to UV through the transparent mask. The obtained mould is then silanized by exposure to TMCS vapor in a low pressure environment during two hours. PDMS with reticulator (1 : 10) is then deposited on the mould. After exposure to vacuum for degassing, the PDMS is reticulated overnight in a 60 °C oven. Finally PDMS with the transferred pattern is then attached to a glass cover by simple contact after surface plasma activation during five minutes. The set-up is heated overnight before use. Flow is induced in the channel by imposing an excess pressure (130 mbar) between channel outlet and inlet and the channel electric resistance is measured using the method discussed above. The time-dependent resistance $R_e(t)$ is plotted in Fig. 4. A first observation is that $R_e(t)$ does exhibit a curvature *versus* time as expected. The corresponding time-derivative of the channel resistance $dR_e(t)/dt$ is plotted in the inset.

As expected from the microchannel design, three regions are indeed observed in the electric resistance, corresponding to the

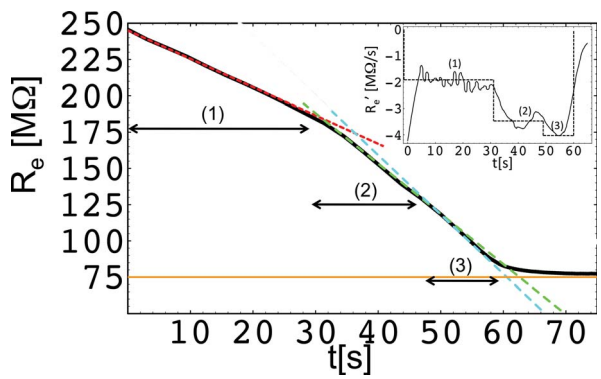

Fig. 4 Channel resistance *versus* time during flux monitoring measurement for the three region channel. The salt concentrations are $c_1 = 0.1$ M and $c_2 = 0.05$ M. The pressure drop is $\Delta P = 130$ mbar. Straight lines are local linear fits of the resistance *versus* time. It corresponds to the variations when the salt front is moving through the channel. In the inset the time derivative of the resistance showing three regions associated with the three different channel widths. The horizontal dashed lines correspond to the values of the slopes measured in the main graph.

three sections of the channel. We have represented in Fig. 4 the expected crossing times corresponding to the motion of the salt front through three different sections of the channel. Accordingly the signal $R_e(t)$ is well fitted by three straight lines. In the first period, the averaged fluid velocity is $\bar{V}_1 = L_1/T_1 = 2.8$ mm s^{-1} and the variation in the electric resistance is 70 MΩ, which is indeed in good quantitative agreement with the expected value at these concentrations. From mass conservation, the velocity in the second period is expected to be $\bar{V}_2 = 3.73$ mm s^{-1}, which is again in good agreement with the measured experimental result. Furthermore, the predicted variations of the channel electric resistance is represented by the second dashed line (2) in Fig. 4 and fits perfectly without any adjustable parameter to our experimental data. Finally, a third region is evidenced in Fig. 4. However the predicted value for the slope for $R_e(t)$ overestimates (in absolute value) the measured one. This actually points to the limitation of the simple analysis made above to obtain quantitative estimates in the present stringent conditions. Relatively long transients, of order 10 s, are indeed observed in Fig.4, inset, which can be ascribed to the lateral diffusion of the salt as the front crosses the sharp intersection between two regions. As shown by Ajdari *et al.*,[18] the transient time for Taylor–Aris dispersion in a shallow geometry is limited by diffusion over the *largest* width. Here one expects therefore $\tau_{\text{transient}} \sim \Delta w^2/D$, with $\Delta w = 50$ μm the change in lateral width: this yields $\tau_{\text{transient}}$ of several seconds, in agreement with the observed value shown in Fig. 4, inset. This transient is of the same order of magnitude as the estimated convective time $L_3/\bar{V}_3 \sim 11$ s in the last region, so that the electric resistance cannot reach a stationary state in this regime. However, beyond quantitative values, the method is at least successful in evidencing the presence of this last region.

Altogether the experimental test of the flux monitoring method shows that it can be used as a diagnostic for variations of the lateral cross-section, even in relatively stringent conditions as considered in the example here – with sharp steps in the section.

As a conclusion, we propose a new experimental method allowing to probe flow rate under pressure-driven flow, inspired from the so-called current monitoring method deviced for electro-osmotic flow characterization. As a result the method allows to measure the hydrodynamic resistance of the channel. The proposed approach is low-cost and easy to implement, without the need for complex integration in the microchannel. This method was shown to allow for efficient characterization of flows in two distinct benchmark set-ups, with dimensions differing by two orders of magnitude. An analytical description allows to rationalize the experimental results and does provide a diagram for its range of applicability in terms of a Peclet number and channel width-to-length aspect ratio, see ESI.† The applicability of this method to characterize a channel with a varying cross-section was also discussed. It is interesting to note that the present method can be directly extended to channels exhibiting branches. For example, for a system exhibiting, say, two asymmetric branches, it is easy to show that the electric resistance will exhibit a piece-wise linear decrease in time, with each period controlled by the time $\tau_i = L_i/v_i$ (L_i the length of the branch i, v_i the fluid velocity in this branch). Since the pressure drop ΔP is the same in the various branches, one may thus extract the hydrodynamic permeability $K_{\text{hyd},i} = v_i/(-\Delta P)$ for each branch and hence estimate the width of the corresponding branch of the

microchannel. The approach can be thus applied to more elaborated geometries, and allow to extract useful information on the hydrodynamic characteristics of the device. The simplicity of the proposed method makes it robust to investigate complex systems. Reversely, if the geometry is known, this method can be used as a viscometer to measure the viscosity of the solution.

References

1 T. Squires and S. Quake, Microfluidics: Fluid physics at the nanoliter scale, *Rev. Mod. Phys.*, 2004, **77**, 977–1026.
2 L. Bocquet and E. Charlaix, Nanofluidics, from bulk to interfaces, *Chem. Soc. Rev.*, 2010, **39**, 1073–1095.
3 M. C. Audry, A. Piednoir, P. Joseph and E. Charlaix, Amplification of electro-osmotic flows by wall slippage: direct measurements on OTS-surfaces, *Faraday Discuss.*, 2010, **146**, 113–124.
4 G. Paumier, J. Sudor, A.-M. Gue, F. Vinet, M. Li, Y. J. Chabal, A. Estève and M. Djafari-Rouhani, Nanoscale actuation of electrokinetic flows on thermoreversible surfaces, *Electrophoresis*, 2008, **29**, 1245–1252.
5 S. Krishnamoorthy, J. Feng, A. Henry, L. Locascio, J. Hickman and S. Sundaram, Simulation and experimental characterization of electro-osmotic flow in surface modified channels, *Microfluid. Nanofluid.*, 2006, **2**, 345–355.
6 Pennathur, Sumita and J. G. Santiago, Electrokinetic Transport in Nanochannels. 2. Experiments, *Anal. Chem.*, 2005, **77**, 6782–6789.
7 G. Tomasz, Elbuken, Caglar, Lee, E. J. Lucy and C. L. Ren, Microfluidic system with integrated electro-osmotic pumps, concentration gradient generator and fish cell line (RTgill-W1)-towards water toxicity testing, *Lab Chip*, 2009, **9**, 3243–3250.
8 X. H. Huang, M. J. Gordon and R. N. Zare, Current monitoring method for measuring the electro-osmotic flow-rate in capillary zone electrophoresis, *Anal. Chem.*, 1988, **60**, 1837–1838.
9 S. Arulanandam and D. Q. Li, Determining zeta potential and surface conductance by monitoring the current in electro-osmotic flow, *J. Colloid Interface Sci.*, 2000, **225**, 421–428.
10 J. L. Pittman, C. S. Henry and S. D. Gilman, Experimental studies of electro-osmotic flow dynamics in microfabricated devices during current monitoring experiments, *Anal. Chem.*, 2003, **75**, 361–370.
11 D. Sinton, C. Escobedo-Canseco, L. Q. Ren and D. Q. Li, Direct and indirect electro-osmotic flow velocity measurements in microchannels, *J. Colloid Interface Sci.*, 2002, **254**, 184–189.
12 R. Venditti, X. C. Xuan and D. Q. Li, Experimental characterization of the temperature dependence of zeta potential and its effect on electro-osmotic flow velocity in microchannel, *Microfluid. Nanofluid.*, 2006, **2**, 493–499.
13 V. Studer, G. Hang, A. Pandolfi, M. Ortiz, W. F. Anderson and S. R. Quake, Scaling properties of a low-actuation pressure microfluidic valve, *J. Appl. Phys.*, 2004, **95**, 393–398.
14 S. J. Williams, C. Park and S. T. Wereley, Advances and applications on microfluidic velocimetry techniques, *Microfluid. Nanofluid.*, 2010, **8**, 709–726.
15 J. Collins and A. P. Lee, Microfluidic flow transducer based on the measurement of electrical admittance, *Lab Chip*, 2004, **4**, 7–10.
16 J. Wu and J. Ye, Micro flow sensor based on two closely spaced amperometric sensors, *Lab Chip*, 2005, **5**, 1344–1347.
17 G. Taylor, Dispersion of soluble matter in solvent flowing slowly through a tube, *Proc. R. Soc. London, Ser. A*, 1953, **219**, 186–203; R. Aris, On the dispersion of a solute in a fluid through a tube, *Proc. R. Soc. London, Ser. A*, 1956, **235**, 67–77.
18 A. Ajdari, Bontoux and H. Stone, Hydrodynamic dispersion in shallow microchannels: the effect of cross-sectional shape, *Anal. Chem.*, 2006, **78**, 387–392.